International Journal of High Speed Electronics and Systems
Vol. 17, No. 3 (2007) 557–566

World Scientific
www.worldscientific.com

HIGHER-ORDER PLASMON RESONANCES IN GAN-BASED FIELD-EFFECT TRANSISTOR ARRAYS

V. V. POPOV[a] and M. S. SHUR

Department of Electrical, Computer, and System Engineering, Rensselaer Polytechnic Institute, Troy, New York 12180, USA,
and RPI/IBM Center for Broadband Data Transfer, CII 9015, Rensselaer Polytechnic Institute, Troy, New York 12180, USA
shurm@rpi.edu

G. M. TSYMBALOV and D. V. FATEEV

Institute of Radio Engineering and Electronics (Saratov Branch), ul. Zelyonaya 38, Saratov 410019, Russia
popov@soire.renet.ru

Terahertz (THz) response spectra of GaN-based field-effect transistor (FET) arrays are calculated in a self-consistent electromagmetic approach. Two types of FET arrays are considered: (i) FET array with a common channel and a large-area grating gate, and (ii) array of FET units with separate channels and combined intrinsic source and drain contacts. It is shown that the coupling between plasmons and THz radiation in the FET array can be strongly enhanced as compared to a single-unit FET. The computer simulations show that the higher-order plasmon modes can be excited much more effectively in the array of FET units with separate channels and combined source and drain contacts then in FET array with a common channel and a large-area grating gate.

Keywords: Field-effect transistor; plasmons; terahertz detection.

1. Introduction

High-frequency response of field-effect transistors (FETs) with two-dimensional (2D) electron channels is strongly affected by plasma oscillations exited in the channel under the gate electrode.[1,2] This phenomenon in its various manifestations can be used for the detection,[3-8] mixing[9-11] and generation[12-17] of terahertz (THz) radiation.

There are two different types of plasma oscillations exist in a FET-like device. They are plasma oscillations excited in either ungated or gated regions of the electron channel. The dispersion relation for ungated plasma oscillation in an infinite 2D electron sheet (with neglect of the electron scattering in 2D electron layer) has a form[18,19]

[a] On leave from: Institute of Radio Engineering and Electronics (Saratov Branch), ul. Zelyonaya 38, Saratov,410019, Russia. Electronic mail: popov@soire.renet.ru

$$\underline{\omega}_p^2 = \frac{e^2 N}{m^* \varepsilon_0 (\varepsilon_1 + \varepsilon_2)} k \,, \tag{1}$$

where $\underline{\omega}_p$ and k are the frequency and wavevector of plasma wave, respectively, N is the areal electron density, ε_0 is the dielectric permittivity of vacuum, ε_1 and ε_2 are the dielectric constants of surrounding materials (substrate and barrier materials, respectively, see Fig. 1), e and m^* are the charge and effective mass of electron, respectively. The values of wavevector k of the ungated plasmons are quantized according to the length of ungated portion of the electron channel. The dispersion described by Eq. (1) is similar to that of gravitational waves on the surface of liquid in a deep basin. Thus this type of plasma waves may be referred to as the "deep water plasmons".[20]

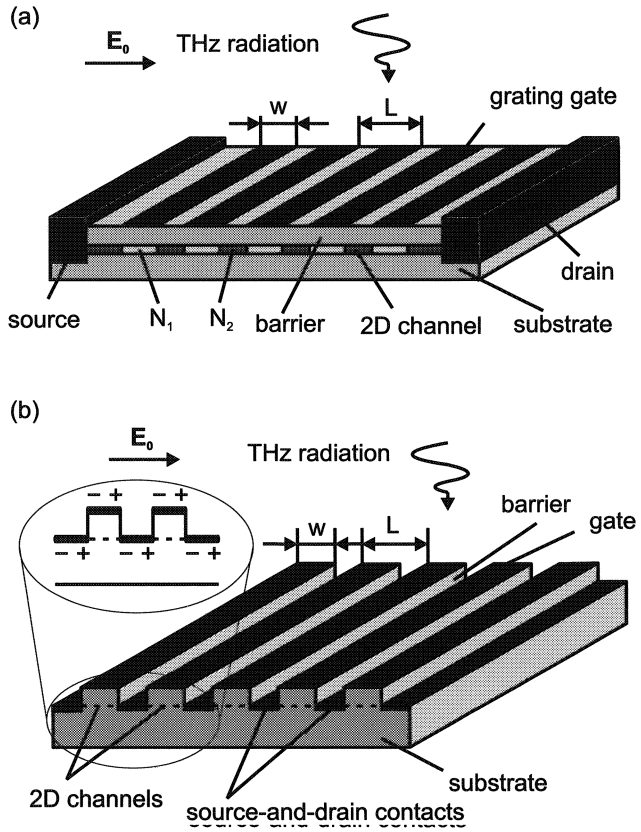

Fig. 1. Schematics of the FET arrays with (a) a common 2D electron channel and a grating gate and (b) with separate electron channels. Polarization of the electric field E_0 of the incident terahertz radiation is shown.

Plasma oscillations of the other type are excited in gated regions of the channel. If the infinite perfectly conductive gate plane is located at distance d from the infinite 2D electron channel then the dispersion relation for this kind of plasma waves is[21]

$$\bar{\omega}_p^2 = \frac{e^2 N}{m^* \varepsilon_0 [\varepsilon_1 + \varepsilon_2 \coth(kd)]} k \,. \tag{2}$$

If the gate plane is close enough to the electron channel, i.e., $kd \ll 1$, one obtains

$$\bar{\omega}_p = \sqrt{\frac{e^2 N d}{m^* \varepsilon_0 \varepsilon_2}} k \,, \tag{3}$$

which means that the plasma waves in the gated region have frequency-independent phase velocity $s = \bar{\omega}_p / k$. The values of the wavevector of the gated plasmons are quantized according to the length of the gate W, $k = n\pi / W$ with n being an integer. However, plasmon modes with even numbers n can not be excited by THz radiation under the gate contact with symmetric boundary conditions at the gate edges (because of zero net dipole moment of such modes). The plasma wave dispersion described by Eq. (3) is similar to that of gravitational waves on the surface of liquid in a shallow basin. Thus this particular type of plasma waves is referred to us the "shallow water plasmons".[1,2] The gated plasmons may be also referred to as the "acoustic plasmons", since their linear dispersion, Eq. (3), similar to that of the acoustic waves.

If $d \ll W$, the areal electron density in the gated region of the channel is related to the gate voltage by the parallel plate capacitor formula

$$N = \frac{\varepsilon_0 \varepsilon_2}{ed} U_0 \,, \tag{4}$$

where $U_0 = U_g - U_{th}$ is the difference between the gate voltage U_g and the channel threshold voltage U_{th}. Then Eq. (3) for the odd plasmon modes acquires a simple form[1,2]

$$\bar{\omega}_p = k \sqrt{\frac{eU_0}{m^*}} \tag{5}$$

with the gated-plasmon phase velocity $s = \sqrt{eU_0 / m^*}$ and $k = (2n-1)\pi / W$ ($n = 1,2,3,...$).

Plasmon modes excited under the gate contact (gated plasmons) are more attractive for practical applications because their frequencies can be effectively tuned by varying the gate voltage. However, simple estimations show that the frequency of the fundamental plasmon mode ($n = 1$) in a GaN-based HEMT may exceed 10 THz only if the gate length is shorter than 100 nm, which sets a limitation for designing the single-gate FET plasmon devices in the high-frequency THz range. (It should be also noted that HEMT's with such a short gate typically has quite long ungated access regions of the 2D electron layer connecting the gated portion of the channel to the source and drain contacts.[22]) Another problem to be solved is how to effectively couple the gated plasmons to THz radiation. Unfortunately, the gated plasmons in a single-gate FET are weakly coupled to THz radiation[23] because: (i) the gated plasmons are strongly screened by the metal gate contact, (ii) they are have a vanishingly small net lateral dipole moment due to their acoustic nature (in this mode, electrons oscillate out-of-phase in the gate contact and

in the channel under the gate, which results in vanishingly small net lateral dipole moment), and (iii) gated plasmons strongly leak into ungated access regions of the channel.[23] Higher-order gated-plasmon modes ($n > 1$) have greater frequencies but even a smaller net dipole moment as compared to the fundamental plasmon mode, and they are more prone to leaking from the gated portion of the channel into the access regions. Hence, the higher-order gated plasmon modes in a single-gate FET can hardly be used for increasing the operation frequency of a single-gate THz plasmonic transistor.

It was suggested in Ref. 23 that the coupling efficiency of gated plasmons to THz radiation can be dramatically enhanced due to their interaction with the ungated portions of the electron channel. A sequence of gated and ungated portions of the channel can be realized, for example, in a FET with a grating gate. In this paper, we calculate the THz plasmon absorptions spectra of the FET with a common channel and a large-area grating gate [see Fig. 1(a)] in frame of the fist principle self-consistent electrodynamic approach and show that the gated-plasmon resonances in such a structure increase by several orders of magnitude due to excitation of plasma oscillations in the ungated portions of the channel. We also show that pronounced higher-order plasmon resonances can be excited in a slit-grating gate FET.

The slit-grating-gate coupler is a conventional tool for exciting the higher-order plasmon modes in a 2D electron channel.[24,25] However, a grating coupler with extremely narrow (sub-100-nm-wide) slits has to be fabricated in order to achieve a measurable strength of the higher-order plasmon resonances[24,25]. Because of that, we suggest in this paper an alternative FET array design with FET units having separate channels and combined intrinsic source and drain contacts [see Fig. 1(b)]. Such a design allows one to effectively excite higher-order plasmon resonances in a structure having the characteristic dimensions of a micron scale. In earlier paper,[26] it was suggested that the coupling between plasmons in the FET channel and THz radiation might be more effective if FET units were arranged in an array. (Also see even earlier relevant paper,[27] where periodic ohmic contacts were alloyed into 2D electron channel producing an array of 2D electron diodes.) It was anticipated[26] that the plasmons in an array of FET's should absorb (or emit) THz radiation at least by a factor of the number of FET units in the array as stronger as a single-unit FET. In a recent paper,[28] we showed that the coupling between plasmons and THz radiation in the FET arrays can be strongly enhanced well beyond that obvious estimation due to a cooperative effect of synchronizing the plasma oscillations in all FET units in the array. In this paper, we demonstrate by computer simulation that intensive higher-order plasmon resonances can be effectively excited in high-frequency THz range (up to 20 THz) in the FET array with separate channels and combined source and drain contacts due to the strong coupling between plasmons and THz radiation. It is shown that in such a device the higher-order plasmon modes are excited much more effectively than in the FET structure with a large-area 2D electron channel coupled to THz radiation by a slit-grating gate.

2. Theoretical Approach

We have calculated the THz plasmon absorption spectra of two different FET arrays shown schematically in Fig. 1 in frame of the first principle self-consistent electrodynamic approach, using the Maxwell equations and the integral equation method developed earlier.[29-31] This approach involves the following steps:

(1) the Maxwell equations are re-written in the Fourier series representation,
(2) using the electrodynamic boundary conditions in the channel and gate planes, the amplitudes of the Fourier harmonics of the oscillating-electron-current density are related to those of the in-plane THz electric field in the gate as well as electron channel planes,
(3) equalizing the sheet electron current density obtained in the previous steps to that in the Ohm's law yields the system of integral equations for the in-plane THz electric field in each (gated and ungated) portion of 2D electron channel as well as in metal contact strips within a period of the structure,
(4) the system of integral equations is solved numerically by the Galerkin method[32] through its projection on an orthogonal set of the Legendre polynomials within the respective interval.

Within this approach we describe the response of electron fluid in each portion of the 2D electron channel, having the equilibrium electron density either N_1 or N_2 [see Fig. 1(a)], by the sheet conductivity in the local Drude model as

$$\sigma(\omega) = i\frac{e^2 N_{1,2}}{m^*(1-i\omega\tau)}, \tag{6}$$

where τ is the electron relaxation time. The sheet electron density under the gate strips N_1 is calculated in the parallel-plate capacitor model by formula Eq. (4) with d being the gate-to-channel distance (the barrier-layer thickness). Calculations were performed for the characteristic parameters of A1GaN/GaN HEMT: $\varepsilon_2 = 9$, $U_{th} = -(3\div8)$ V, $d = (8\div20)$ nm. Surface conductivity of the metal gate strips as well as the source and drain contacts in the FET array structure shown in Fig. 1(b) was assumed to be 2.5 S. Numerical calculations showed that the plasmon absorption spectra do not change noticeably at small (compared to the saturation current) DC currents through the channel (if one neglects the effect of the gated-channel-portion length modulation by the drain current, which does not change the physics of the effects under consideration). Because of that all numerical results below are presented for zero DC drain current. Notice that Eq. (6) describes an inductive admittance arising from a kinetic inductance of the 2D electron system responding to the total in-plane THz electric field (and having a resistive contribution caused by the electron scattering in the 2D channel). A capacitive contribution (which is necessary to produce a resonance in the whole system responding to the external THz electric field) describing the oscillating-charge accumulation in the system is provided by the gate-to-channel capacitance and is accounted for in our approach self-consistently by applying the proper electrodynamic boundary conditions in the channel and gate planes.

3. Grating-Gate FET with a Common Channel

Figure 2 shows the THz absorption spectra of AlGaN/GaN HEMT with a common channel and a large-area grating gate [see Fig. 1(a)] having 1-μm-wide grating-gate strips for three different grating-gate-slit widths and zero gate voltage. These results demonstrate quite pronounced and well-resolved higher-order plasmon resonances even at room temperature in the structure with sub-micron slits. For narrower slits the higher resonances are excited with larger amplitudes, since narrow grating-gate slits generate strong higher Fourier harmonics of the incident THz wave. As a result, quite pronounced higher-order plasmon resonances may be excited at high THz frequencies up to 7th resonance at about 10 THz (not shown in Fig. 2).

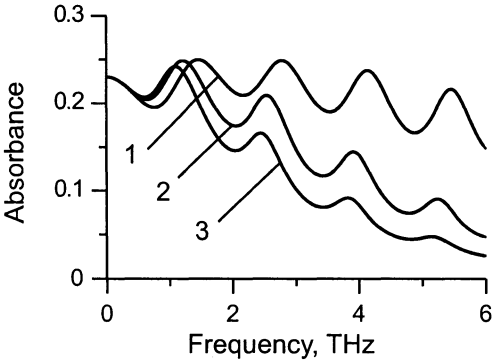

Fig. 2. Absorption spectra of AlGaN/GaN HEMT with 1-μm-wide grating-gate strips for three different slit widths: 0.1 μm (curve 1), 0.3 μm (curve 2) and 0.5 μm (curve 3) at room temperature ($\tau = 2.27\times10^{-13}$ s) for zero gate voltage. $U_{th} = -3$ V, $d = 8$ nm.

The equidistant spectrum of plasmon resonances shown in Fig. 2 is characteristic of the acoustic-like dispersion, see Eq. (3), which evidences the excitation of the gated-plasmon modes in the structure (the ungated-plasmon modes with their dispersion given by Eq. (1) have much higher frequencies). The radiative damping and dissipation of plasmon oscillations contribute comparably to the total linewidth of the plasmon resonance in the FET with a slit-grating gate, which makes all plasmon resonances stronger. The maximum absorbance of 0.5 at the plasmon resonance is reached when the radiative and dissipative contributions to the resonance linewidth become equal (this condition for the maximum absorption can be also readily understood as matching the free-space impedance to the FET impedance at the plasmon resonance).[30] It is worth noting that for narrow slit widths the frequencies of plasmon resonances are the multiples of $2\pi/L$ and not the multiples of π/W as for a single-gate FET structure [see Eq. (3)]. This leads to a blue shift of all plasmon resonances seen in Fig. 2 for shorter periods of the structure. The calculations show that all plasma resonances *become weaker by two orders of magnitude* when the electron density under the grating-gate openings tends to zero. This fact demonstrates a crucial role of the ungated portions of the channel in excitation of the gated plasmons.

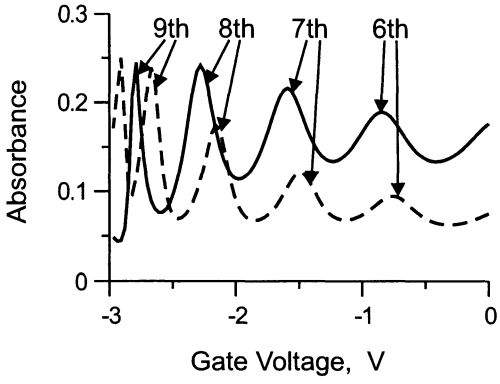

Fig. 3. The same as in Fig. 2 as a function of the gate voltage for two different slit widths: 0.1 μm (solid curve), 0.2 μm (dashed curve) at frequency 6.86 THz. Plasmon mode numbers are indicated.

Figure 3 shows the terahertz absorption of A1GaN/GaN HEMT with 1-μm-wide grating-gate strips and sub-micron grating-gate slits as a function of the gate voltage. The most intriguing result here is that the intensity of higher-order plasmon resonances (up to 9th order) increases at more negative gate voltage. It happens because the radiative damping of higher-order plasmon modes increases with increasing the electron density modulation along the electron channel (hence, a value of the radiative damping becomes closer to that of the dissipative damping of plasmons, which ensures more favorable condition for excitations of the plasmon resonances).[30] Notice also that the plasma resonances excited at more negative gate voltages exhibit a narrower resonance linewidth, ΔU_g. The more negative the resonant value of U_g, the narrower the resonance is. One can easily understand this fact by performing the differentiation of Eq. (5):

$$\Delta U_g \propto \Delta\bar{\omega}_p \sqrt{U_g - U_{th}}\,, \tag{7}$$

where $\Delta\bar{\omega}_p$ is the linewidth of the plasmon resonance in the frequency domain. Obviously, for a given $\Delta\bar{\omega}_p$, ΔU_g tends to zero when U_g approaches the threshold voltage U_{th}.

4. FET Array with Separate 2D Electron Channels

In Fig. 4 the calculated THz absorption spectra of the FET array with separate electron channels [see Fig. 1(b)] are shown for two different array periods and two different gate-strip width for zero gate voltage. (One can easily imagine a biasing scheme allowing to apply the identical gate and drain bias voltage to every FET in the array.) These results demonstrate that in such a structure, the intensive fundamental and all higher-order plasmon resonances up to the 8th resonance at 20 THz (not shown in Fig. 4) can be excited with comparable amplitudes even at room temperature. All resonances are shifted to higher frequencies for narrower gate-strip width as predicted by Eq. (5).

Plasma oscillations in all unit cells of the periodic FET array are excited with the same phase (and amplitude) dictated by the phase (and amplitude) of the incoming THz

wave. Even without the incoming THz wave, the plasmons, once excited (either by a thermal or stimulated mechanism), oscillate in phase in all unit cells of the FET array shown in Fig. 1(b) because the side metal contacts with high conductivity act as effective synchronizing elements between adjacent unit cells. Applying a mechanical analogy, one may think of rigid crossbars connecting oscillating springs arranged in a chain. Therefore, the plasma oscillations in the FET array behave as a single plasmon mode distributed over the entire area of the array. The formation of this cooperative mode ensures strong coupling between plasmons in the FET array and external THz radiation.[28]

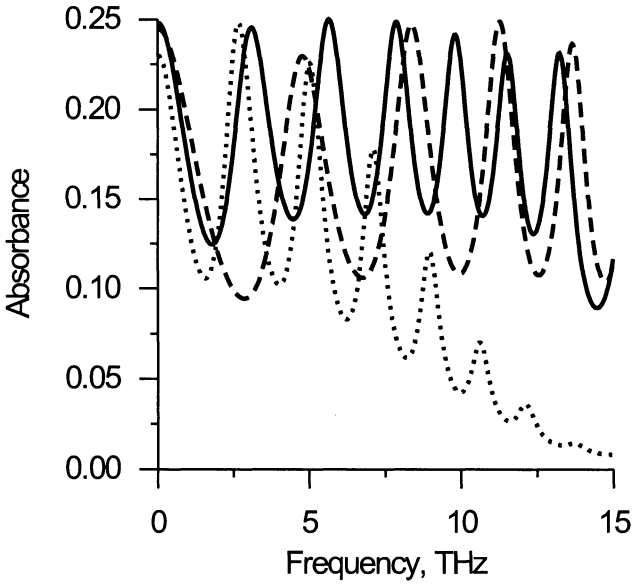

Fig. 4. Terahertz absorption spectra of the array of AlGaN/GaN HEMT's with separate channels for two different gate lengths of each HEMT unit, 0.8 μm (solid curve) and 0.5 μm (dashed curve), at room temperature ($\tau = 2.27 \times 10^{-13}$ s) and zero gate voltage. Period of the array is 1.2 μm. Dotted curve shows the THz absorption spectrum of AlGaN/GaN HEMT with a homogeneous 2D electron channel and a slit-grating gate with the period 0.9 μm and the slit width 0.1 μm. $U_{th} = -7.5$ V, $d = 20$ nm (from Ref. 28).

One can see from Fig. 4 that, although there is no by far a sub-100-micron characteristic lateral dimension in the FET array with separate electron channels, the higher-order plasmon modes are excited much more effectively in such a structure than in a FET structure with a common electron channel and a grating gate having the 100-nm-wide slits (see Sec. 3 and the dotted curve in Fig. 4). The physical mechanism of the higher-order plasmon mode excitation is entirely different in these two different structures. In the grating-gate coupler, narrow slits generate strong higher Fourier harmonics of the incident THz field with wavevectors $k = 2n\pi/L$, where L is the period of the grating gate with n being an integer. Then these strong Fourier harmonics excite higher-order plasmon modes with the same wavevectors in the channel when the frequency of the incoming THz wave coincides with the plasmon mode frequency. In contrast, in the FET array with separate channels, the incoming THz radiation induces the

oscillating charges of opposite sign across the vertical (typically sub-100-nm-wide) gap between the gate and side contacts at each edge of the gate contact in every FET unit [see inset in Fig. 1(b)]. These oscillating charges induce the electric fields with the same symmetry as in the plasmon modes excited under the gate contact with symmetric boundary conditions at the gate-contact edges. Hence, plasmon modes are effectively excited when their eigen-frequency coincide with the frequency of the incoming THz radiation.

5. Conclusions

It is shown that the coupling between plasmons and THz radiation in the FET arrays with either joint or separate 2D electron channels can be strongly enhanced as compared to a single-gate FET. Computer simulations show that the higher-order plasmon modes can be excited much more effectively in the FET array with separate channels as compared to the FET array with a common 2D electron channel and a slit-grating gate. Such enhancement is due to a cooperative effect of synchronizing the plasma oscillations in all separate channels in the FET array. These results open a gateway to designing the FET plasmonic devices in the high-frequency THz range up to 15 THz and even higher.

Acknowledgments

This work has been supported in part by the Russian Foundation for Basic Research (Grant No. 06-02-16155), Russian Academy of Sciences program "Quantum Nanostructures", by ONR (Program Managers Scott Steward and Dave Masters) and CRDF (Grant No. 2681).

References

1. M. Dyakonov and M. Shur, *IEEE Trans. Electron Devices* **43,** 380 (1996).
2. M.S. Shur and J.-Q.Lü, *IEEE Trans. Microwave Theory and Techniques* **48**, 750 (2000).
3. W. Knap, Y. Deng., S. Rumyantsev, J.-Q. Lu, M. S. Shur, C. A. Saylor, and L. C. Brunel, *Appl. Phys. Lett.* **80**, 3433 (2002).
4. X. G. Peralta, S. J. Allen, M. C. Wanke, N. B. Harff, J. A. Simmons, M. P. Lilly, J. A. Reno, P. J. Burke, and J. P. Eisenstein, *Appl. Phys. Lett.* **81**, 1627 (2002).
5. A. Satou, I. Khmyrova, V. Ryzhii, and M. S. Shur, *Semicond. Sci. Technol.* **18**, 460 (2004).
6. F. Teppe, W. Knap, D. Veksler, A. P. Dmitriev, V. Yu. Kachorovskii, S. Rumyantsev, and M. S. Shur, *Appl. Phys. Lett.* **87,** 052107 (2005).
7. E. A. Shaner, M. Lee, M. C. Wanke, A. D. Grine, J. L. Reno, and S. J. Allen, *Appl. Phys. Lett.* **87**, 193507 (2005).
8. D. Veksler, F. Teppe, A. P. Dmitriev, V. Yu. Kachorovskii, W. Knap, and M. S. Shur, *Phys. Rev. B* **73**, 125328 (2006).
9. V. Ryzhii, I. Khmyrova, A. Satou, P. O. Vaccaro, T. Aida, and M. S. Shur, *J. Appl. Phys.* **92**, 5756 (2002).
10. A. Satou, V. Ryzhii, I. Khmyrova, and M.S. Shur, *J. Appl. Phys.* **95**, 2084 (2005).
11. M. Lee, M. C. Wanke, and J. L. Reno, *Appl. Phys. Lett.* **86**, 033501 (2005).
12. W. Knap, J. Lusakowski, T. Parenty, S. Bollaert, A. Cappy, V. V. Popov, and M. S. Shur, *Appl. Phys. Lett.* **84**, 2331 (2004).

13. T. Otsuji, M. Hanabe, and O. Ogawara, *Appl. Phys. Lett.* **85**, 2119 (2004).
14. Y. Deng, R. Kersting, J. Xu, R. Ascazubi, X.-C. Zhang, M. S. Shur, R. Gaska, G. S. Simin, M. A. Khan, and V. Ryzii, *Appl. Phys. Lett.* **84**, 70 (2004).
15. N. Dyakonova, F. Teppe, J. Lusakowski, W. Knap, M. Levinshtein, A. P. Dmitriev, M. S. Shur, S. Bollaert, and A. Cappy, *J. Appl. Phys.* **97**, 114313 (2005).
16. V. Ryzhii, A. Satou, and M. S. Shur, *Phys. Stat. Sol. (a)* **202**, 113 (2005).
17. N. Dyakonova, A. El Fatimy, J. Lusakowski, W. Knap, M. I. Dyakonov, M.-A. Poisson, E. Morvan, S. Bollaert, A. Shchepetov, Y. Roelens, Ch. Gaquiere, D. Theron, and A. Cappy, *Appl. Phys. Lett.* **88**, 141906 (2006).
18. R. H. Ritchie, *Phys. Rev.* **106**, 874 (1957).
19. F. Stern, *Phys. Rev. Lett.* **18**, 546 (1967).
20. M. Dyakonov and M. S. Shur, *Appl. Phys. Lett.* **87**, 111501 (2005).
21. A. V. Chaplik, *Zh. Eksp. Teor. Fiz.* **62**, 746 (1972) [*Sov. Phys. JETP* **35**, 395 (1972)].
22. T. Parenty, S. Bollaert, J. Mateos, X. Wallart, and A. Cappy, *Proc. 13th Int. Conf. Indium Phosphide and Related Materials (IPRM 2001)*, Nara, Japan, 626 (IEEE, New York, 2001).
23. V. V. Popov, O. V. Polischuk, and M. S. Shur, *J. Appl. Phys.* **98**, 033510 (2005).
24. T. N. Theis, *Surface Science* **98**, 515 (1980).
25. E. Batke, D. Heitmann, and C. W. Tu, *Phys. Rev. B* **34**, 6951 (1986).
26. M. I. Dyakonov and M. S. Shur, *Appl. Phys. Lett.* **67**, 1137 (1995).
27. S. J. Allen, F. Derosa, R. Bhat, G. Dolan, and C. W. Tu, *Physica B+C* **134**, 332 (1985).
28. V. V. Popov, G. M. Tsymbalov, D. V. Fateev, and M. S. Shur, *Appl. Phys. Lett.* **89**, 123504 (2006).
29. O. R. Matov, O. F. Meshkov, and V. V. Popov, *Zh. Eksp. Teor. Fiz.* **113**, 988 9 (1998) [*JETP* **86**, 538 (1998)].
30. V. V. Popov, O. V. Polischuk, T. V. Teperik, X. G. Peralta, S. J. Allen, N. J. M. Horing, and M. C. Wanke, *J. Appl. Phys.* **94**, 3556 (2003).
31. V. V. Popov, G. M. Tsymbalov, and N. J. M. Horing, *J. Appl. Phys.* **99**, 124303 (2006).
32. G. Korn, T. Korn, *Mathematical Handbook*, 2nd ed. (McGraw-Hill, New York, 1968).